Electronic Supplementary Material (ESI) for Physical Chemistry Chemical Physics.

Supplementary Information
Plastic deformation and twinning mechanisms in magnesian calcites: a non-equilibrium computer simulation study

Sanha Lee, Gøran Brekke Svaland, Fernando Bresme

Department of Chemistry
Imperial College London

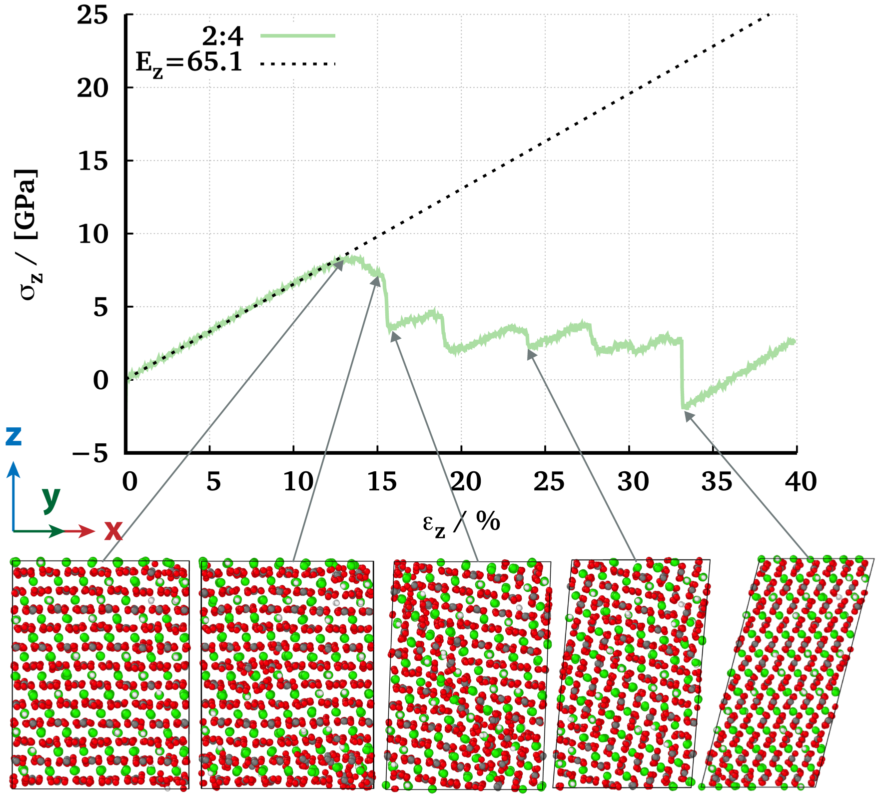

Figure 1: Stress *vs.* strain curve for magnesian calcite of 2:4 Mg:Ca ratio. Elastic coefficient E_z obtained from line fit of elastic regime at strain rate $s = 0.2\,s^{-1}$.

Table 1: Force field parameters for $(Mg,Ca)CO_3$.

Buckingham		A(kcal/mol)	r(Å)	C(kcal/mol/Å)
Ca	O	72908.9819425084	0.271511	0
Ca	C	2767265033.43952	0.12	0
Mg	O	51374.9602439005	0.255294	0
Mg	C	1949939915.70948	0.112832	0
O	O	1472189.58683767	0.198913	643.3662442171
Charges		q_{Ca},q_{Mg} (e)	q_C (e)	q_O (e)
		+2	+1.123282	-1.041094

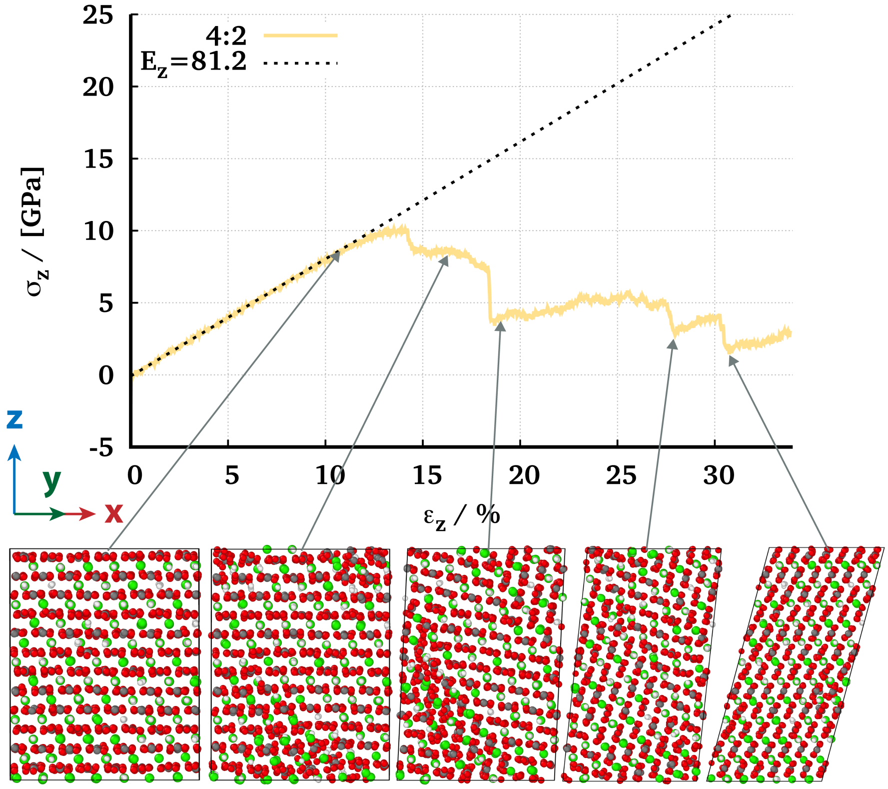

Figure 2: Stress *vs.* strain curve for magnesian calcite of 4:2 Mg:Ca ratio. Elastic coefficient E_z obtained from line fit of elastic regime at strain rate $s = 0.2\,s^{-1}$.

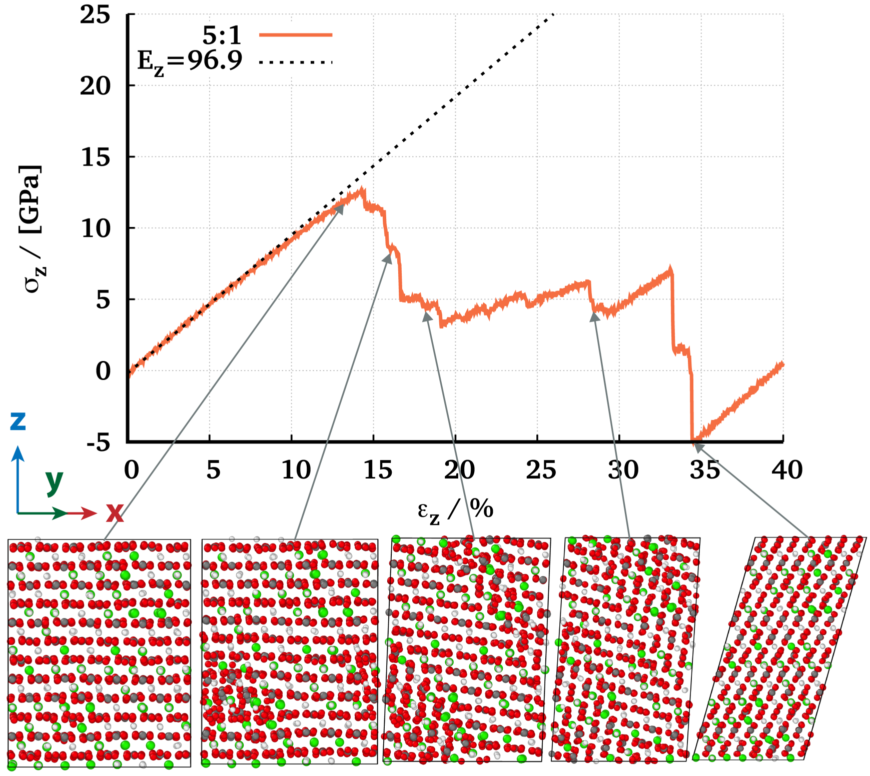

Figure 3: Stress *vs.* strain curve for magnesian calcite of 5:1 Mg:Ca ratio. Elastic coefficient E_z obtained from line fit of elastic regime at strain rate $s = 0.2\,s^{-1}$.

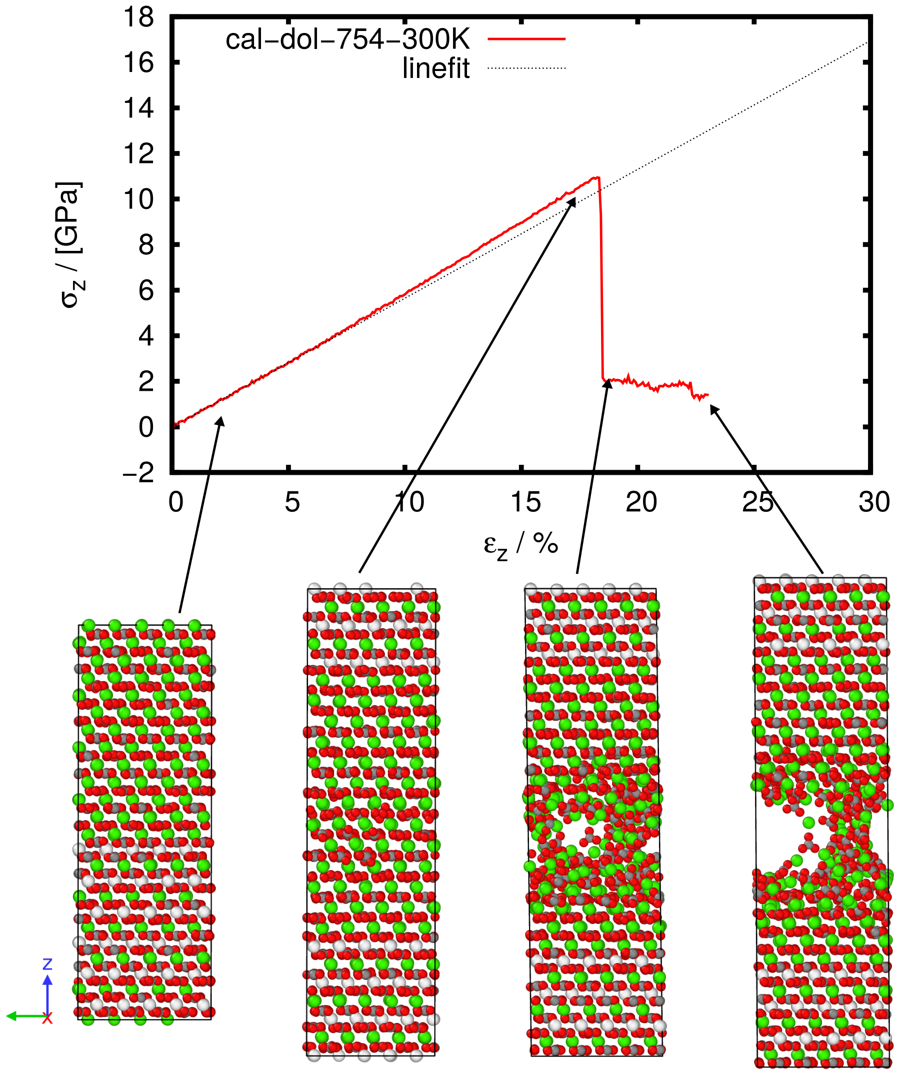

Figure 4: Stress *vs.* strain curve for a system with calcite and dolomite interface along the c-axis. Elastic coefficient $E_z = 56\,\mathrm{GPa}$ obtained from line fit of elastic regime at strain rate $s = 0.1\,s^{-1}$. In comparison, for pure calcite we obtain $E_z = 56\,\mathrm{GPa}$, and for dolomite we obtain $E_z = 66\,\mathrm{GPa}$.

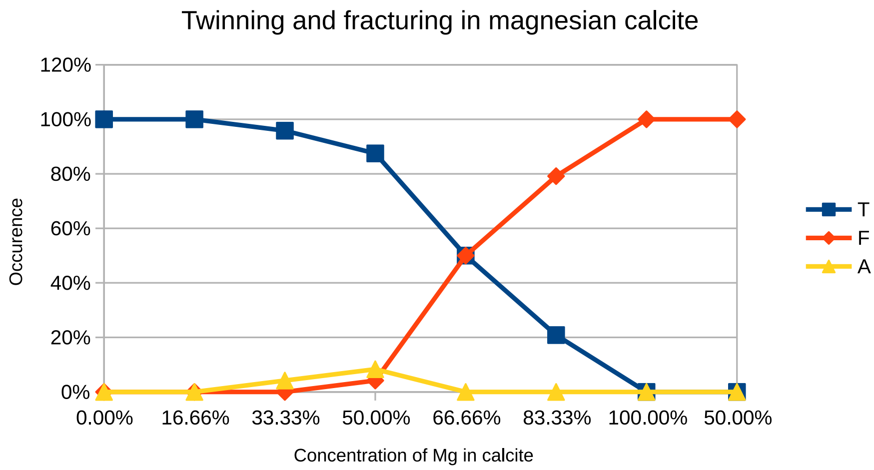

Figure 5: Graphical representation of the data in Table 1 in the main article. Probability of deformation twinning (T), alternate twinning (A) and shear fracture (F) during applied uniaxial strain along c-axis in magnesian calcites. The data were obtained from four independent simulations at each of the six strain rates: $(0.15, 0.2, 0.25, 0.3, 0.4 \text{ and } 1.0)\,\mathrm{s}^{-1}$. For the pure cases, calcite, magnesite and dolomite, data were obtained from one trajectory for each strain rate. Values at 50 % Mg concentration to the right corresponds to dolomite.

Strain Rate	0.15				0.2				0.25				0.3				0.4				1			
0:6	T				T				T				T				T				T			
1:5	T	T	T	T	T	T	T	T	T	T	T	T	T	T	T	T	T	T	T	T	T	T	T	T
2:4	T	T	T	T	T	T	T	T	T	T	T	T	T	T	T	T	T	T	T	T	T	A	T	T
3:3	T	T	T	T	T	T	T	T	A	T	T	T	F	T	T	T	A	T	T	T	T	T	T	T
4:2	T	F	F	F	T	T	F	T	F	F	T	F	F	F	T	T	F	T	F	T	F	T	T	T
5:1	T	F	F	F	T	F	F	F	T	F	F	F	T	F	F	F	F	F	F	F	T	F	F	F
6:0	F				F				F				F				F				F			
dolomite	F				F				F				F				F				F			

Figure 6: Summary of observed deformation twinning (T) and (A) and shear fracture (F) distribution for uniaxial stress along the c-axis. Results obtained from independent simulations at each of the six strain rates: $(0.15, 0.2, 0.25, 0.3, 0.4 \text{ and } 1.0)\,\mathrm{s}^{-1}$.

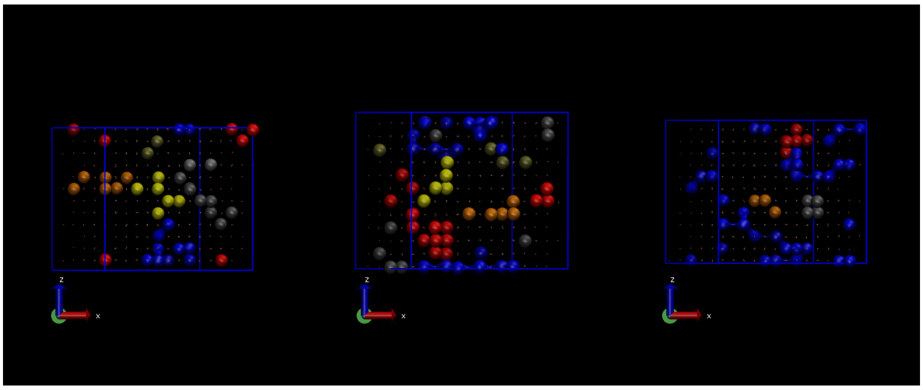

Figure 7: Mg^{2+} clusters in different colors from Voronoi tessellation at 1:5 Mg:Ca ratio. Largest cluster shown as surface. Ca^{2+} are shown as points. Magnesium ions belonging to the same cluster are represented in the same color.

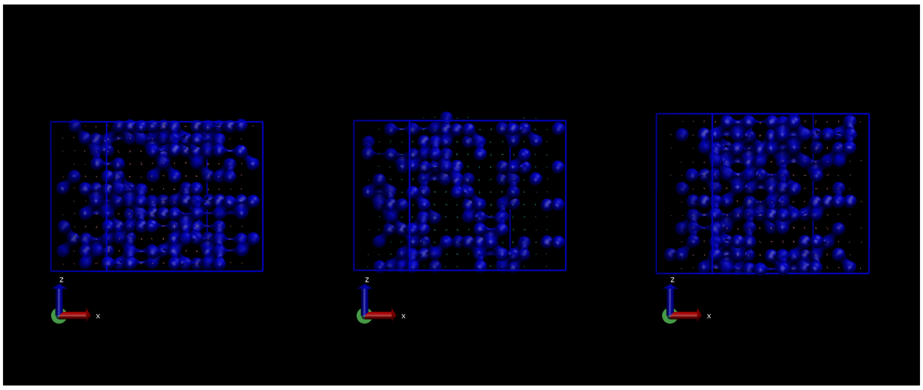

Figure 8: Mg^{2+} percolating cluster from Voronoi tessellation at 2:4 Mg:Ca ratio. Cluster shown as surface. Ca^{2+} are shown as points.

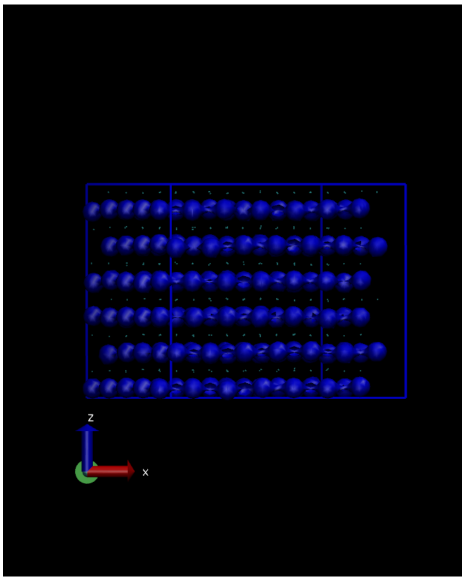

Figure 9: Mg^{2+} percolating cluster from Voronoi tessellation in dolomite. Cluster shown as surface. Ca^{2+} are shown as points.

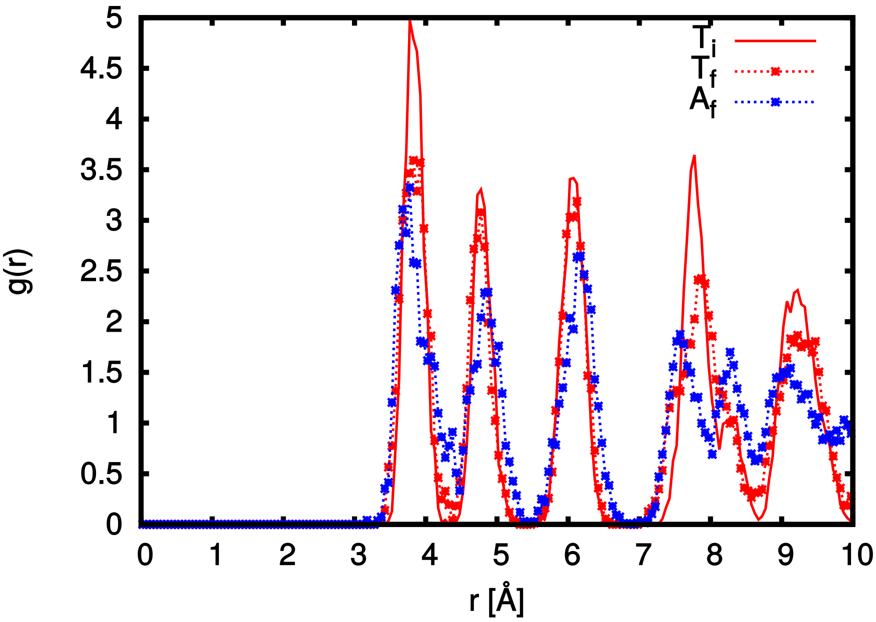

Figure 10: Radial distribution function of Ca^{2+} and Mg^{2+} ions in the initial i, and final f configuration of T and A type deformation. A_i and T_i are the same structure.

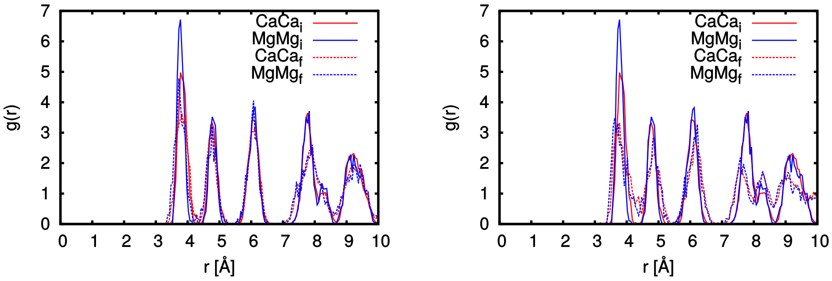

Figure 11: Radial distribution function of Ca^{2+} ion pairs and Mg^{2+} ion pairs in the initial i, and final f configuration of T (left) and A (right) type deformation.

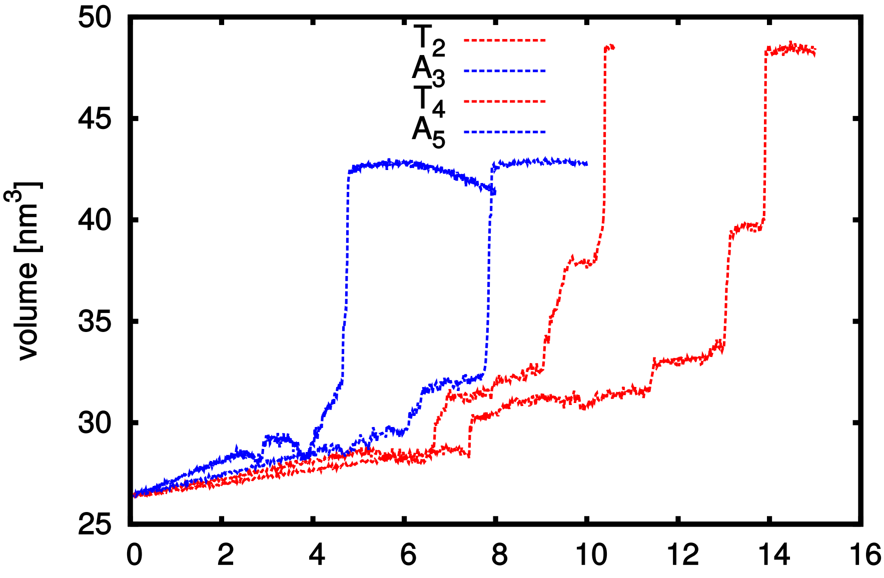

Figure 12: Volume of the simulation cell as a function of time for A and T type deformations for four different simulations: 2, 3, 4 and 5. Simulations were performed at 3:3 Mg:Ca ratio of randomly incorporated Mg^{2+}.

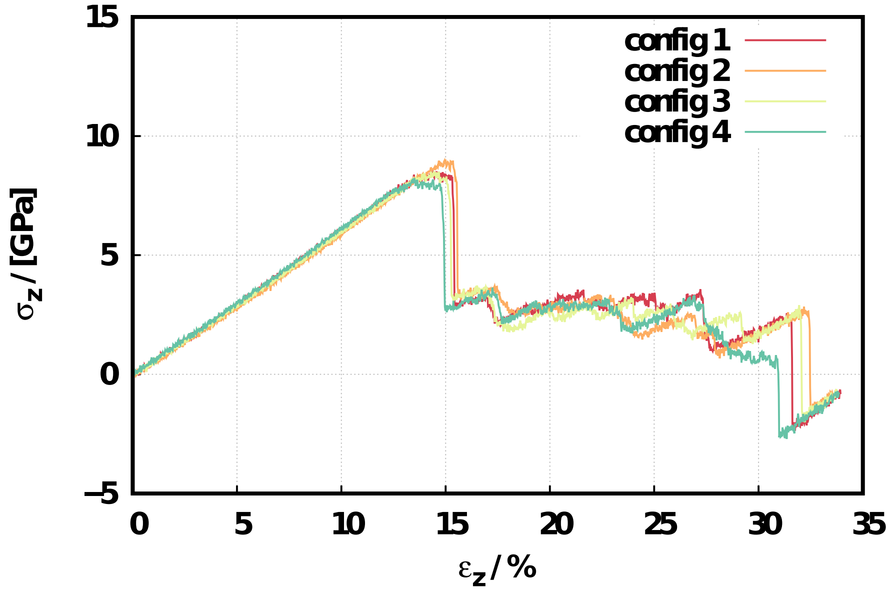

Figure 13: Deformation response at 1:5 Mg:Ca ratio for 4 random configurations (config) 1,2,3 and 4.

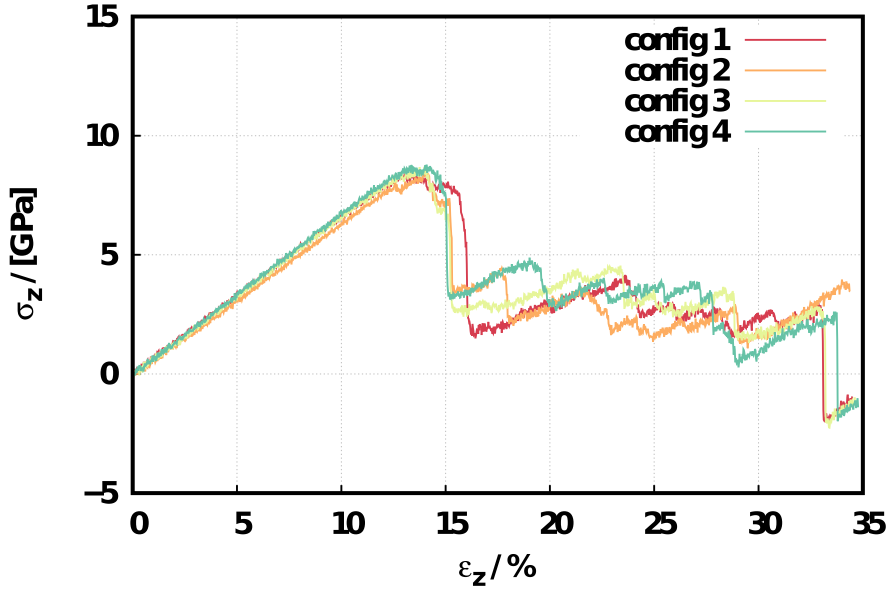

Figure 14: Deformation response at 2:4 Mg:Ca ratio for 4 random configurations (config) 1,2,3 and 4.

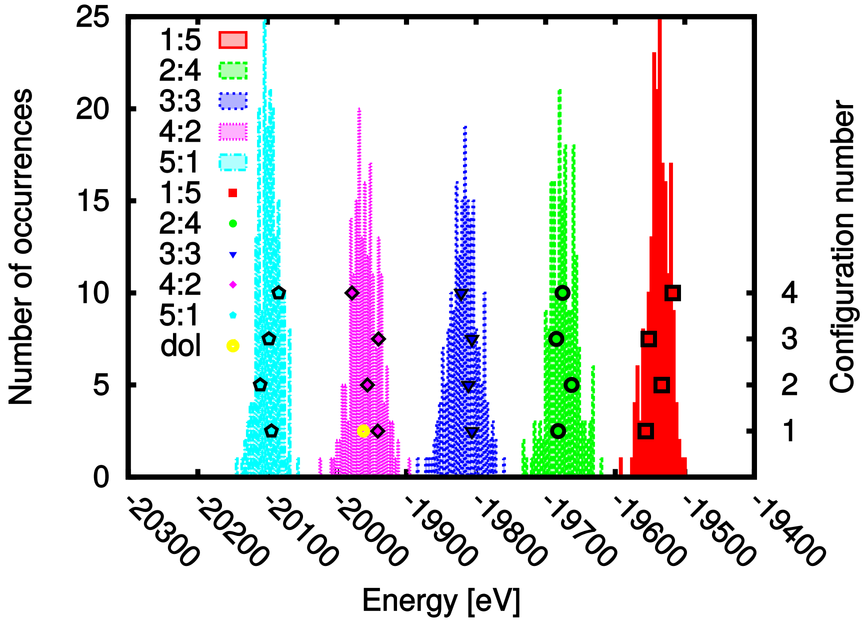

Figure 15: Histogram of distribution of 200 potential energies of configurations randomly generated at 1:5, 2:4, 3:3, 4:2 and 5:1 Mg:Ca ratios. Standard deviations of the generated energies were of the order $\sigma_E/\langle E\rangle = 0.01$. Points show potential energies of 4 selected configurations discussed in the results in the main paper. “dol” (yellow point) is for dolomite.

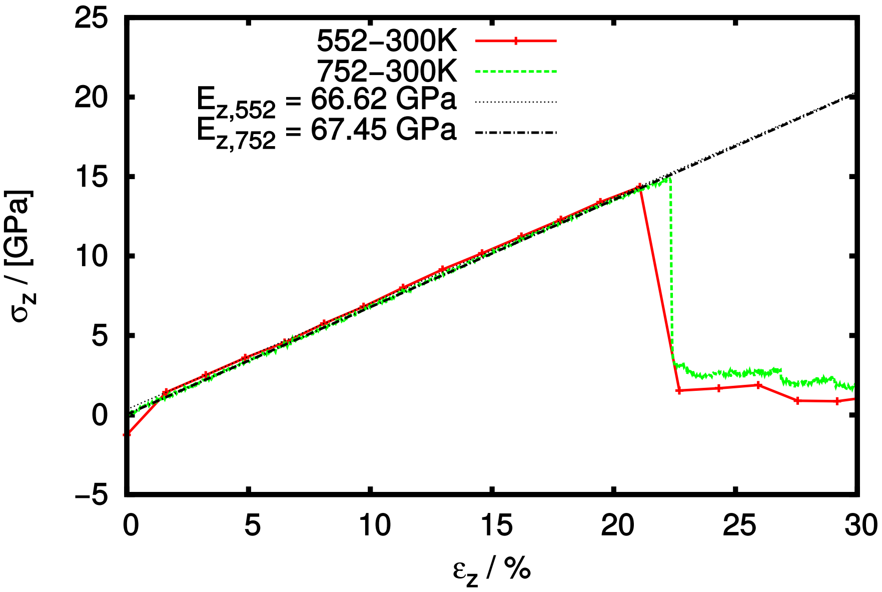

Figure 16: Stress *vs.* strain curve for two different periodic supercells of $5\times5\times2$ and $7\times5\times2$ unit cells for dolomite. Elastic coefficients E_z obtained from line fit in the elastic regime at strain rate $s = 0.2\,s^{-1}$.

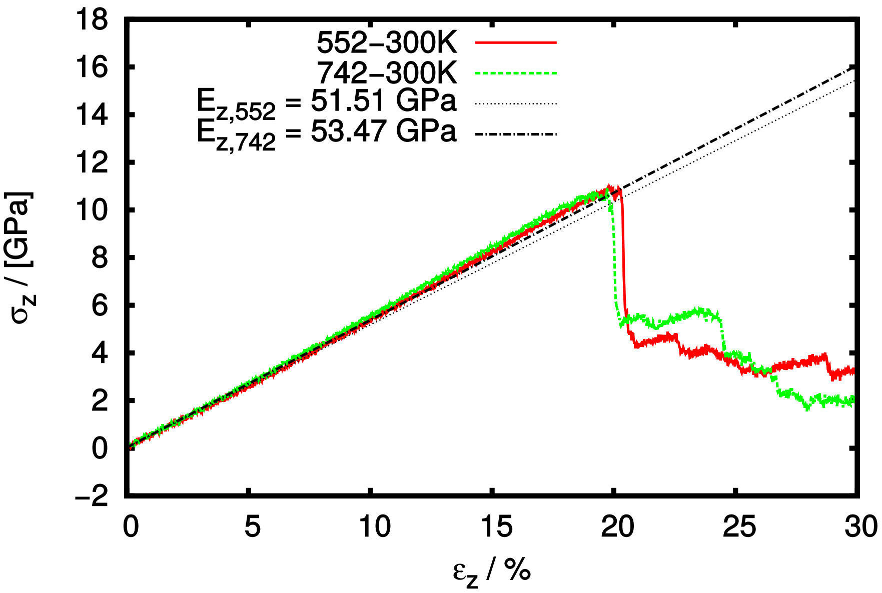

Figure 17: Stress *vs.* strain curve for two different periodic supercells of $5\times5\times2$ and $7\times4\times2$ unit cells for magnesian calcite at 3:3 Mg:Ca ratio. Elastic coefficients E_z obtained from line fit in the elastic regime at strain rate $s = 0.2\,s^{-1}$.